J. Phys. B: At. Mol. Opt. Phys. **41** (2008) 165206 (7pp) doi:10.1088/0953-4075/41/16/165206

Positron and electron collisions with anti-protons in strong magnetic fields

Jennifer L Hurt, Patrick T Carpenter, Christine L Taylor and F Robicheaux

Department of Physics, Auburn University, AL 36849-5311, USA

Received 3 June 2008, in final form 21 July 2008
Published 8 August 2008
Online at stacks.iop.org/JPhysB/41/165206

Abstract
Recent simulations of anti-hydrogen production rely on the rate that anti-protons are slowed in positron plasmas. These plasmas are typically cold and in strong magnetic fields. This paper describes Classical Trajectory Monte Carlo calculations of the momentum transfer cross sections for positron collisions with anti-protons. We also give results for electron collisions with anti-protons. For the typical temperatures and magnetic fields in the anti-hydrogen experiments, the dominant slowing mechanism is the close, non-perturbative collisions; all previous calculations of the slowing rate are for situations where the perturbative collisions dominate. These cross sections are converted into a slowing rate as a function of magnetic field and temperature. For the parameter range of current interest, we find this to be an extraordinarily simple function.

1. Introduction

Recently, two groups [1, 2] reported the formation of anti-hydrogen ($\bar{H}$) by having anti-protons ($\bar{p}$) traverse a positron (e^+) plasma. The e^+'s and $\bar{p}$'s are trapped in the same region of space using a nested Penning trap geometry [3]. In this geometry, a strong magnetic field along the trap axis prevents the charged particles from escaping radially. A series of electrodes then hold both the e^+'s and $\bar{p}$'s in different positions along the trap.

Simulations were performed of the $\bar{H}$ production [4]. These simulations included the motion of the $\bar{p}$, the three-body recombination which gives the $\bar{H}$, the positron collision with the highly excited $\bar{H}$ which gives de-excitation to more deeply bound states and the slowing of the $\bar{p}$ due to interaction with the plasma waves [5]. A correct description of the slowing of the $\bar{p}$ is crucial because the interplay of the slowing and the rate of $\bar{H}$ formation determines the centre-of-mass speed of the $\bar{H}$. If the $\bar{p}$ loses energy rapidly to collisions with positrons or to interaction with plasma waves, then the $\bar{H}$ will tend to form after considerable slowing has taken place. The formulation of $\bar{p}$ slowing in [5] is not accurate when the $\bar{p}$'s speed is comparable to or less than the thermal speed of the positrons. This casts some doubt on the accuracy of the calculated velocity distribution of $\bar{H}$ because it is just this range of velocities where recombination occurs.

The velocity of the $\bar{H}$ formed in the experiments has been roughly measured in [6, 7]. These measurements were consistent with the velocity distribution from the simulation of [4]. A later simulation involving a second charge exchange found that the velocities in [8] might have been lower than what was suggested in the original measurement, but still quite hot compared to the temperature of the positrons.

The next goal of the two anti-hydrogen experiments is to trap some of the $\bar{H}$. This will only be possible if the $\bar{H}$ centre-of-mass energy is less than $\sim 2/3$ K when it reaches the ground state. Thus, the slowing of a $\bar{p}$ in a cold, magnetized plasma is an important aspect in understanding the production of trappable $\bar{H}$. However, neither experiments nor simulations are accurate for the low-velocity population of $\bar{H}$ and it is unclear whether an experimentally interesting fraction of $\bar{H}$'s is present at low energy.

The purpose of this paper is to compute the momentum transfer cross section of light species interacting with $\bar{p}$'s in strong magnetic fields. Although this is an old problem that has been investigated many times, we could not find calculations that would be accurate for the range of parameters in the anti-hydrogen experiments. References [5, 9, 10] compute the slowing of an ion in a magnetized electron plasma including the effect of plasma waves; however, these results are not expected to be accurate when the ion velocity is comparable to or less than the thermal velocity of the electrons because the interaction is computed perturbatively where the emphasis is on large impact parameter collisions. Reference [11] investigated the quantum scattering

of electrons from ions but for magnetic fields many orders of magnitude larger than those considered here. There have been several calculations of the modification of the collisions between electrons and ions in strong fields for situations where the dominant collisions are those at large impact parameters [12–14]. In this region, perturbation theory can be used to obtain the scattering with a strong magnetic field. However, simple considerations show that the close, non-perturbative collisions dominate the momentum transfer cross section for the parameters of the anti-hydrogen experiments. Finally, there have been full calculations of electron-ion scattering in strong magnetic fields [15–17] in the spirit of this paper. However, the focus of these papers is on the interesting physics of the scattering; there were no results of total scattering parameters (e.g. momentum transfer cross sections) presented in these papers.

One of the general features of these calculations was that the ion motion perpendicular to the field is damped out substantially faster than the parallel motion with the magnetic field. This can be rationalized from the interaction of a magnetized electron travelling past a stationary positive ion. If the impact parameter is a few times larger than the cyclotron radius, the electron will travel past in a helical path. The impulse to the ion along the field will be nearly zero because impulse arising during the electron's approach almost exactly cancels the impulse as the electron recedes. However, the impulse perpendicular to the field adds over the whole of the path. Also, the electron cannot recoil perpendicular to the field which means it behaves as if it has a large mass with regards to the perpendicular motion. This effect was seen in the simulations of [4].

In this paper, we are solely interested in the momentum transfer to the $\bar{\mathrm{p}}$ along the magnetic field: since the perpendicular components of the velocity thermalize much faster than the parallel component, whether a $\bar{\mathrm{p}}$ loses sufficient energy to be trappable will mainly depend on the slowing rate parallel to the magnetic field. Also, the thermalization of the perpendicular components of the $\bar{\mathrm{p}}$ velocity are more accurately described by the previous calculations even though they use perturbative techniques. We will show that the momentum transfer along the magnetic field is mainly due to close, non-perturbative collisions. In this case, perturbative techniques do not give a sufficiently accurate solution. We use a full numerical solution of the *classical equations of motion* to obtain accurate momentum transfer parallel to the magnetic field over the full range of impact parameters.

We also perform calculations for the interaction of $\bar{\mathrm{p}}$'s with electrons because this case has a particularly simple expression for the momentum transfer cross section. The interaction with positrons is more complicated due to the attractive interaction which causes some trajectories to pass close to the $\bar{\mathrm{p}}$ and give chaotic scattering [15–17]. We use the results of our atomic calculation to compute the slowing rate due to single particle scattering when the $\bar{\mathrm{p}}$ velocity is comparable to or less than the thermal velocity of the light species. It must be emphasized that this scattering does *not* include losses due to interaction with plasma waves which is an open question at these energies.

One of the positive features of a perturbative treatment is that the scattering parameters can be expressed as (relatively) simple formulae. Typically, these involve the impact parameter, the velocity of the projectile and the energy and phase of the cyclotron motion. Unfortunately, perturbation theory is not applicable for the $\bar{\mathrm{H}}$ experiments.

To see whether the perturbative or non-perturbative collisions play the largest role, the distance scale given by the Coulomb interaction can be compared to the distance scale for the collision. Suppose a light particle is launched at a charge fixed in space so that the impact parameter is b and the velocity parallel to the magnetic field is $v_\parallel$. In order for the collision to be perturbative, the potential energy at the distance of closest approach should be much smaller than the kinetic energy. This gives the relation: $e^2/(4\pi\varepsilon_0 b) \ll (1/2)mv_\parallel^2$. Because of the magnetic field, the charge has a cyclotron motion which gives it an adiabatic invariant [18]. This means there is almost no modification to the motion if the timescale for the collision $(b/v_\parallel)$ times the frequency of the motion ($\omega_{\mathrm{cyc}} = eB/m$) is much larger than 1.[1] This leads to the relation that little scattering occurs if: $b \gg mv_\parallel/(eB)$. Combining these two relations means that the non-perturbative collisions will dominate for speeds $v_\parallel < (e^3B/[2\pi\epsilon_0 m^2])^{1/3}$. For a 1 T field, this gives $v_\parallel \sim 4.5 \times 10^4$ m s^{-1} which corresponds to a temperature of approximately 70 K. In the $\bar{\mathrm{H}}$ experiments, the goal is to reach positron and electron temperatures of approximately 4 K. Thus, the non-perturbative collisions will be most important for the $\bar{\mathrm{H}}$ experiments.

Another consideration is whether the calculations can be performed with the $\bar{\mathrm{p}}$ fixed in space. If we were interested in the thermalization of the cyclotron motion of the $\bar{\mathrm{p}}$, we would need to include that motion in our calculation. Since we are only interested in the motion along the field, it is not clear whether or not that motion is important. A simple way to compute the momentum transfer to the $\bar{\mathrm{p}}$ is to take the negative of the momentum transfer to the positron or electron. Because the close, non-perturbative collisions dominate, it seems likely that the two calculations will yield similar results. We have performed the calculation with the $\bar{\mathrm{p}}$ fixed in space and with it having its correct, physical mass in order to check the importance of this effect.

In this paper, we first describe some of the basic features of the calculation, including approximations and their estimated contribution to inaccuracies in our results. We then show the results from electron collisions with the $\bar{\mathrm{p}}$'s and then positron collisions with the $\bar{\mathrm{p}}$'s. We then convert momentum transfer cross section into slowing rates as a function of the $\bar{\mathrm{p}}$ velocity parallel to the magnetic field.

2. Computational method

All of the calculations are performed in a strong magnetic field. We will take the magnetic field to be in the z-direction and x, y or r, θ will be used to denote positions perpendicular to this field.

[1] Perturbative expressions for the change in perpendicular velocity contain the Bessel function, $K_1(\omega_{\mathrm{cyc}}b/v_\parallel)$, which has the asymptotic form $K_1(x) \sim \sqrt{\pi/(2x)}\exp(-x)$ for large x.

All of the calculations reported in this paper use the Classical Trajectory Monte Carlo method. We solve for the full motion of the particles using the classical Hamilton's equation in Cartesian coordinates. This is an approximation to the extent that quantum effects are unimportant. We do not have a way of estimating the size of this error because the quantum calculations are prohibitively large. We do not expect this to be an important effect because the situations we investigate correspond to large impact parameters compared to the wavelength of the light particle. Also, we average over velocities, impact parameters, etc and the averaging process tends to reduce the size of quantum effects. As an example, a positron in a 1 T field has $\hbar\omega_{\rm cyc} = 1.3$ K compared to the minimum expected temperature of 4 K for these experiments; thus, even the cyclotron motion will have several quanta. One gauge of the error can be obtained from figure 3 where our calculations show that strong scattering occurs out to ~400 nm. The number of quantum states for an electron confined to a circular *area* with radius 400 nm and kinetic energy less than 4 K is roughly 350. Thus, there are several available quanta in all directions so correspondence between the classical and quantum results should be more accurate than the inaccuracies of our final classical result.

We used an adaptive step–size, Runge–Kutta algorithm [19] to solve our ordinary differential equations. Although the algorithm is fourth order, it does not preserve the constants of the motion. We performed two types of convergence checks. For a sampling of parameters, we performed the calculation several times with an increasingly stringent accuracy parameter until our convergence level was achieved. Secondly, we checked the level of change in all of the conserved quantities (e.g. energy, canonical angular momentum, ...) to ensure the error was not too large. The number of rejected trajectories leads to an estimated error from the numerical solution of Hamilton's equations of less than 1% for the total cross sections.

The slowing rate due to single particle collisions can be obtained from the momentum transfer cross section. In a Classical Trajectory Monte Carlo simulation (for example, see [20]), the distribution of initial conditions is determined by the parameter being studied. We computed the momentum transfer by launching the light particle at an initial distance z_i with a random initial x_i, y_i; the x_i, y_i are each chosen from a flat distribution within the range $-L/2$ to $L/2$. The size of L was determined numerically by performing a series of calculations with increasing L until the final results were converged. We chose the light particle to have thermal velocity distribution in the x, y direction, but the velocity along the field was chosen to be a fixed quantity. The $\bar{\rm p}$ was started at the position (0, 0, 0) with 0 velocity parallel to the field. In some of the calculations, we held the $\bar{\rm p}$ fixed in space and in others we allowed the $\bar{\rm p}$ to have a thermal distribution perpendicular to the field and have a finite mass.

The momentum transfer along the field is simply the change in momentum at the end of the run. It can be found from either the $\bar{\rm p}$ or the light particle because the total momentum along the field is a conserved quantity. The momentum transfer cross section in the z-direction is

$$\sigma_{p_z} = L^2\langle\Delta p_z\rangle/p_{z,i}, \qquad (1)$$

where $p_{z,i}$ is the initial momentum of the light particle in the z-direction, L^2 is the area through which the light particles are flowing and the $\langle\Delta p_z\rangle$ is the average momentum transfer for that ensemble.

We performed convergence checks on the momentum transfer cross section with respect to the number of trajectories. We increased the number of trajectories until the fractional variance of $\langle\Delta p_z\rangle$ was roughly 1%. Similarly, we checked the convergence with respect to L by increasing it until the accuracy was roughly 1%. Convergence with respect to L is not completely obvious. The reason is that Coulomb interactions tend to give logarithmic singularities for momentum transfer cross sections. However, this is not a problem for a strong magnetic field. The cyclotron motion causes the spatial integrals to converge [18]. The long-range contribution to the momentum transfer is orders of magnitude smaller than the contribution from close collisions.

One of the main problems in accurately computing the momentum transfer cross section is the slow convergence with respect to the z-range of the calculation. This becomes a problem because the CPU time is proportional to the length in z in the calculation. We found that stopping each trajectory so that the magnitude of the force in the z-direction was the same at the beginning and end of the trajectory greatly increased the speed of convergence with respect to z_i. Also, the approximation that the cyclotron motion was an adiabatic invariant for $|z| > |z_i|$ greatly increased the speed of convergence.

As a final test, we computed the momentum transfer cross section using the change in momentum of the light particle in two different kinds of calculations. In one calculation, we allowed the $\bar{\rm p}$ to move and have a perpendicular temperature equal to the perpendicular temperature of the light particles. In the other calculation, we held the $\bar{\rm p}$ fixed in space. The average momentum along the field lost by the light particle was within a few percent in both cases.

3. Electron scattering

In figure 1, we show the momentum transfer to the $\bar{\rm p}$ as a function of the impact parameter of the electron for an initial electron speed of 2×10^4 m s^{-1}. In both calculations, the perpendicular temperature of the electron is 4 K and the electron has an initial parallel velocity of $v_{z,i}$. In one calculation, the $\bar{\rm p}$ is fixed in space whereas the $\bar{\rm p}$ has the physical mass in the second calculation. In the finite mass calculation, the $\bar{\rm p}$ has a perpendicular temperature of 4 K and the initial conditions are chosen so that it is at the origin at the time $z_i/v_{z,i}$. The two calculations have the same general features. There is a region where the momentum transfer is large and is approximately $2m_{\rm e}v_{z,i}$; this value arises for elastic reflection of the electron. Over a small region of impact parameter the momentum transfer rapidly drops to 0. As a point of reference, the arrow marks the impact parameter where the perturbative estimate of the momentum transfer starts becoming exponentially small.

This can be understood from simple arguments. When the impact parameter is less than $\sim 2e^2/\left(4\pi\varepsilon_0 m v_{z,i}^2\right)$, then the

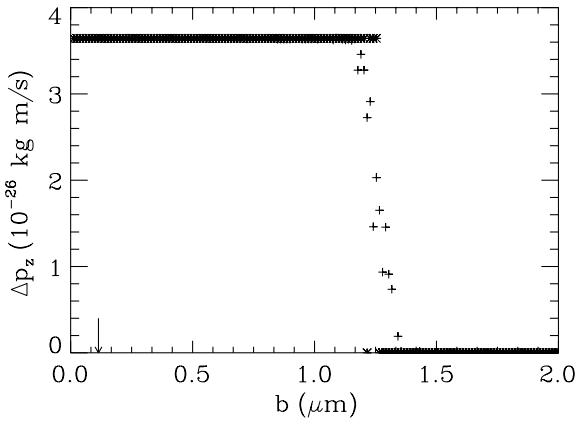

Figure 1. The average momentum transfer to the $\bar{p}$ from electrons with initial velocity of 20 km s^{-1} along the field as a function of the impact parameter. The magnetic field is at 1 T and the perpendicular temperature of the electrons is 4 K. The $*$ is for the $\bar{p}$ fixed in space, while the + is for the $\bar{p}$ having the correct mass and 4 K for the perpendicular temperature.

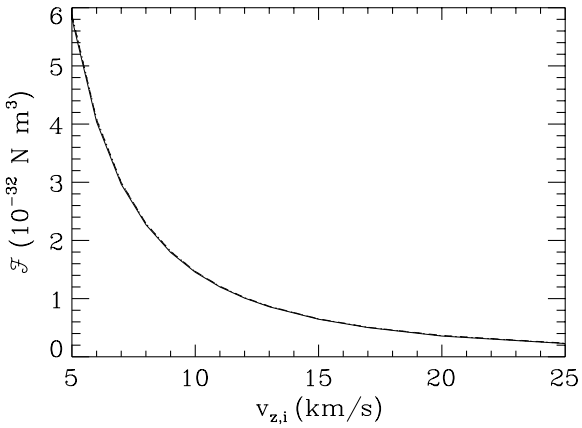

Figure 2. The force per unit density exerted on a $\bar{p}$ from electrons in a 1 T magnetic field with a perpendicular temperature of 4 K as a function of the initial parallel velocity of the electrons. There are three curves: (a) an approximation from simple energy arguments, (b) a numerical calculation with the $\bar{p}$ fixed in space and (c) a numerical calculation with the $\bar{p}$ having the correct mass and 4 K for the perpendicular temperature.

electron does not have enough energy to surmount the repelling potential from the $\bar{p}$ and is reflected back. Since the $\bar{p}$ is much more massive than the electron and it is moving slowly, the electron finishes with approximately the same kinetic energy it started with. When the electron has impact parameter greater than $\sim 2e^2/(4\pi\varepsilon_0 m v_z^2)$, then it has enough energy to pass by the $\bar{p}$. Again, the electron tends to finish with roughly the same kinetic energy it started with because the $\bar{p}$ is slow and heavy. This gives a momentum transfer of approximately 0. It is only in a small range of impact parameter near this cutoff that the momentum transfer is between 0 and $2m_e v_{z,i}$. The transition is mostly due to the motion of the $\bar{p}$: there are some trajectories where the $\bar{p}$ moves sufficient distance in the calculation so the electron's impact parameter at $z = 0$ can (randomly) be larger than the cutoff impact parameter (no reflection) or smaller than the cutoff (reflection).

Instead of the momentum transfer cross section, we have found it useful to present the results in terms of the momentum transfer rate which we are taking to be the momentum transfer cross section times v_z times $p_{z,i}$:

$$\mathcal{F}(v_z) = v_z L^2 \langle \Delta p_z \rangle, \tag{2}$$

which has units of force times volume. If you have a beam of electrons with density n_e impinging on a stationary $\bar{p}$, then $\mathcal{F} n_e$ is the average force on the $\bar{p}$.

For electrons, the momentum transfer rate is approximately given by

$$\mathcal{F} \simeq \frac{e^4}{2\pi\varepsilon_0^2 m v_z^2}, \tag{3}$$

where e is the electron charge and m is the mass of the electron. In figure 2, we show the calculated momentum transfer rate. The plotted results are at three levels of approximation. The dotted line uses the full equations of motion for both the $\bar{p}$ and the electron, the solid line uses the full equation of motion for the electron but the $\bar{p}$ is held fixed in space and the dashed line is the approximation of equation (3). From this graph, it is clear that the physical mass of the $\bar{p}$ is not important and that the simple result from conservation of energy gives an accurate approximation to the full result. The agreement between the simple energy argument and the full numerical calculation shows that the perturbative scattering is not relevant at these energies and fields.

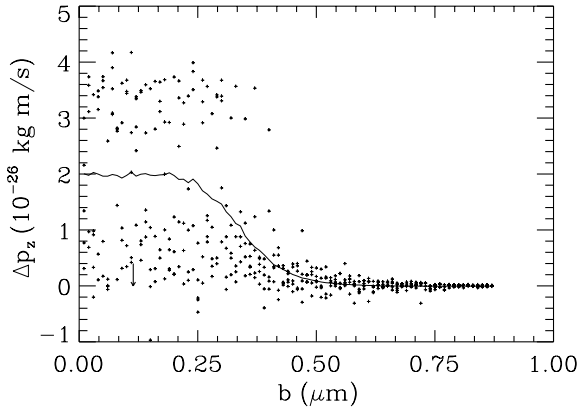

Figure 3. The average momentum transfer to the $\bar{p}$ from positrons with initial velocity of 20 km s^{-1} along the field as a function of the impact parameter (solid line). The symbols show the momentum transfer for individual trajectories (only a small fraction of those used in the calculation are shown). The magnetic field is at 1 T and the perpendicular temperature of the positrons is 4 K.

4. Positron scattering

4.1. Fixed $v_{z,i}$

In figure 3, we show the momentum transfer to the $\bar{p}$ as a function of the impact parameter of the positron for a positron with an initial v_z of 2×10^4 m s^{-1}. The perpendicular temperature of the positron is 4 K. For this calculation, the $\bar{p}$ is fixed in space. Unlike the electron case, the scattering gives a random momentum transfer depending on the phase of the cyclotron orbit. The small + are some of the individual

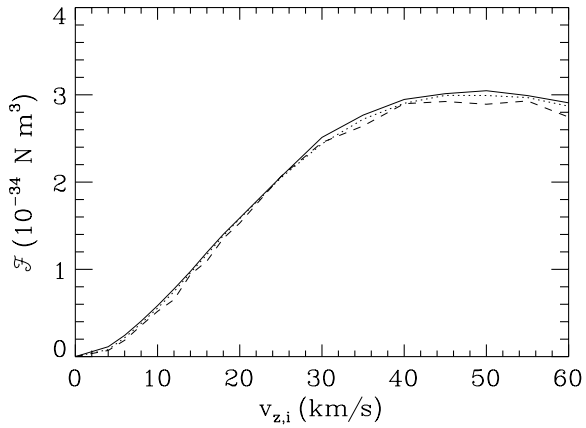

Figure 4. The force per unit density exerted on a $\bar{p}$ from positrons in a 1 T magnetic field as a function of the initial parallel velocity of the positrons. There are three perpendicular temperatures of the positrons: 4 K (solid line), 8 K (dotted line) and 16 K (dashed line).

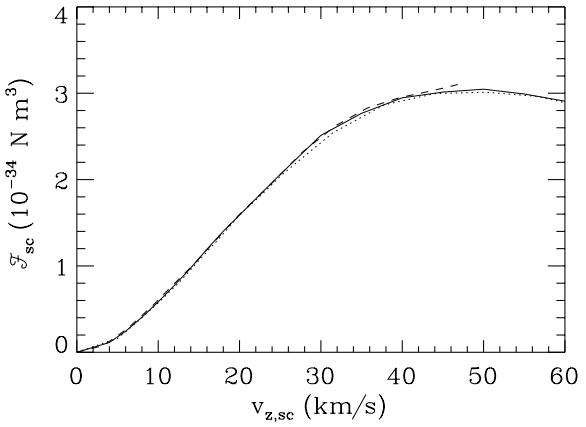

Figure 5. Same as figure 4 but all curves are for the same perpendicular temperature, 4 K. There are three different magnetic fields: 1 T (solid line), 1/2 T (dotted line) and 2 T (dashed line). The results have been scaled so that $v_{z,sc} = v_z/(B/T)^{1/3}$ and $\mathcal{F}_{sc} = \mathcal{F}(B/T)^{2/3}$.

calculations and the solid line is the average momentum transfer at each impact parameter. Since this is the same velocity as the electron in figure 1, one might expect that the momentum transfer would be bounded between 0 and 3.64×10^{-26} kg m s^{-1}. However the actual range extends to negative numbers and above the value of $2mv_{z,i}$. This is because energy can be removed from the cyclotron motion in the close collisions of the positron with the $\bar{p}$. This can lead to situations where the positron speed after the collision is greater than that before the collision. As a point of reference, the arrow marks the impact parameter where the perturbative estimate of the momentum transfer starts becoming exponentially small.

Another interesting feature of figure 3 is that the average momentum cross section substantially differs from 0 for a smaller range of impact parameters. Also, the average momentum transfer at small impact parameter is roughly 1/2 the value for electrons. The momentum transfer cross section for positrons is substantially smaller than that for electrons for velocities less than 50 km s^{-1}.

Figure 4 shows the $\mathcal{F}$ versus the initial velocity of the positrons for a temperature of 4 K, 8 K and 16 K in the cyclotron motion. For this calculation, the $\bar{p}$ is fixed in space. Unlike the case for the electrons, the average force on the $\bar{p}$ goes to 0 as the positron speed along the field decreases to 0. The reason for this is that the range of impact parameters that contribute to scattering becomes finite as the positron velocity decreases to 0 while the momentum available from the positron decreases. If the temperature of the cyclotron motion is nonzero, there is always a finite amount of momentum available from the scattering. However, the scattering rate has an additional factor of v_z which means the average force goes to 0 in this limit. Note this is completely different than the scattering from electrons where $\mathcal{F}$ diverges as v_z goes to 0; the strong dependence on the sign of charge of the projectile is another indication that the perturbative region of scattering is not important.

Another striking feature is the fact that the perpendicular temperature does not play a strong role in the value of $\mathcal{F}$. There is a consistent trend for the higher temperatures to have a lower force, but the differences are barely outside of the estimated uncertainty in our calculation. Our calculations for a finite mass $\bar{p}$ match those shown in figure 4 to within 5%.

Figure 5 shows the $\mathcal{F}$ versus the initial velocity of the positrons for a temperature of 4 K but with different magnetic field strengths. The results shown are for magnetic fields of 1 T, 1/2 T and 2 T with the 1/2 and 2 T results scaled to show the similarity to the 1 T result. The classical equations of motion can be scaled. If the motion is represented by the scaled position $\vec{\rho} = B^{2/3}\vec{r}$, the scaled velocity $\vec{v} = B^{-1/3}\vec{v}$ and scaled energy $\varepsilon = B^{-2/3}E$, then the motion is independent of B when the starting value of $\vec{\rho}$ and $\vec{v}$ are the same. From figure 5, it is clear that the scaling is quite good even though the perpendicular energy is not being scaled. This is because $\mathcal{F}$ only weakly depends on the perpendicular energy.

One of the more important features of figures 4 and 5 is the large region of velocities where the force is roughly linear: a couple km s^{-1} to roughly 30 km s^{-1}. A perfectly linear relation dependence of $\mathcal{F}$ on the incident velocity can arise from a scattering situation where the incident particle can only move in one dimension, the scatterer has a size that decreases like $1/\sqrt{v_{z,i}}$, and the fraction that scatter is independent of velocity. In looking at the scattering shown in figure 3 but for different initial velocities, we find that $\langle \Delta p_z \rangle$ near $b = 0$ is roughly proportional to $v_{z,i}$; this means that roughly the same fraction are scattered independent of initial velocity of the positrons. We also find that the region over which the scattering is large decreases with increasing incident velocity and the decrease is roughly proportional to $1/\sqrt{v_{z,i}}$ over this velocity range. This has important consequences for the rate of slowing in a thermal plasma as discussed in the following section.

4.2. Thermal average

In the experiments that are attempting to make and trap $\bar{H}$, the $\bar{p}$'s slow in a positron plasma. Thus, the relevant quantity is from the thermal average over the positron collisions. If the $\bar{p}$

has a velocity V_z along the magnetic field, the drag force can be written as

$$F_{\text{drag}} = -MV_z n\gamma(V_z, B, T), \tag{4}$$

where M is the mass of the $\bar{\text{p}}$, n is the positron density and $\gamma(V_z, B, T)$ is the slowing rate per unit density which depends mainly on the $\bar{\text{p}}$'s velocity V_z, the magnetic field, and the positron temperature, T.

In the previous section, we showed how the results can be scaled so we will focus on the V_z and T dependence of γ. Taking the positrons to have a Maxwell–Boltzmann distribution in the rest frame, the slowing rate can be computed from

$$\gamma = \frac{1}{MV_z}\sqrt{\frac{m}{2\pi k_{\text{B}}T}}\int_0^\infty \mathcal{F}(v_z) \times \left(\exp\left[-\frac{m(v_z - V_z)^2}{2k_{\text{B}}T}\right] - \exp\left[-\frac{m(v_z + V_z)^2}{2k_{\text{B}}T}\right]\right) \mathrm{d}v_z, \tag{5}$$

where k_{B} is the Boltzmann constant, m is the positron mass and T is the positron temperature. For small V_z the difference in exponentials is proportional to V_z with a correction of order V_z^3. Thus, γ has little dependence on the $\bar{\text{p}}$'s velocity for small V_z.

In performing the integral for γ, we found an extraordinary result. To within 10%, we found

$$\gamma \simeq \frac{4.3 \times 10^{-12}}{B(\text{T})}\ \text{m}^3\ \text{s}^{-1} \tag{6}$$

with B(T) being the magnetic field in tesla; this expression was in good agreement with the numerical calculation for the full range of parameters that we can check which is the range of $|V_z| < 10$ km s^{-1}, temperature between 4 K and 32 K and magnetic field between 1/2 T and 2 T. This result probably extends to a larger range. The dependence of γ on B is a simple result of the scaling discussed in the previous section. The lack of dependence on V_z arises from the definition of γ; upon expanding the difference of the exponentials, the next-order term in V_z is approximately $mV_z^2/6k_{\text{B}}T$ which is less than 1/9 for the range $|V_z| <$ 10 km s^{-1}. The very small dependence on temperature is the most surprising aspect of this equation, but it can be understood from velocity dependence seen in figures 4 and 5.

For the restrictions in the previous paragraph, the approximation

$$\gamma \simeq \int_0^\infty \sqrt{\frac{m}{2\pi k_{\text{B}}T}}\mathcal{F}(v_z)\exp\left[-mv_z^2/2k_{\text{B}}T\right]2\frac{mv_z}{Mk_{\text{B}}T}\,\mathrm{d}v_z \tag{7}$$

arises by taking only the lowest-order term in V_z. When the temperature is in the range of 4–16 K, the exponential drops to $1/e$ at 11–22 km s^{-1}. An examination of figures 4 and 5 shows that the $\mathcal{F}(v_z)$ is roughly linear from a couple km s^{-1} to roughly 30 km s^{-1} which is the region that mostly contributes to the integral. The integral above has no temperature dependence in the situation that $\mathcal{F}(v_z)$ is perfectly proportional to v_z because all terms contain factors of $v_z/\sqrt{T}$.

5. Application

We can use the slowing rate from the previous section to estimate γ from the ATHENA and ATRAP experiments. In [4], we used a density of 2.5×10^{14} m^{-3}, temperature of 15 K and a magnetic field of 3 T for the calculation to model the ATHENA experiment and 4×10^{13} m^{-3}, 4 K and 5.4 T for the calculation to model the ATRAP experiment. Both of these experiments were in the temperature range given in the previous section but the magnetic fields are somewhat higher. However, we expect the expression will still give a good estimate of the slowing rate. Using the expression from the previous section gives $F_{\text{drag}} = -360$ HzMV_z for the ATHENA experiment and $F_{\text{drag}} = -32$ HzMV_z for the ATRAP experiment. Thus, if the main slowing is due to individual collisions with positrons then the slowing was much faster in the ATHENA experiment than in the ATRAP experiment.

6. Conclusions

We performed calculations of the scattering of electrons and positrons from $\bar{\text{p}}$'s in a strong magnetic field. The purpose was to understand the mechanism that controls this process and obtain a simple relation that could be used to estimate the slowing in ongoing experiments at CERN. We have found that non-perturbative collisions dominate the momentum transfer to the $\bar{\text{p}}$'s and, thus, large-scale Classical Trajectory Monte Carlo calculations are needed to obtain usable results. Furthermore, we found that to a good approximation the slowing rate per unit density is inversely proportional to the magnetic field and has very little temperature dependence in the range of interest. Our calculations only include single particle effects; thus, it will be important to have calculations of the energy lost to plasma waves in order to fully understand $\bar{\text{p}}$ slowing in these cold, highly magnetized, positron plasmas.

Acknowledgment

This work was supported by the Office of Fusion Energy Sciences, U.S. Department of Energy.

References

[1] Amoretti M *et al* (ATHENA Collaboration) 2002 *Nature* **419** 456
[2] Gabrielse G *et al* (ATRAP Collaboration) 2002 *Phys. Rev. Lett.* **89** 213401
[3] Gabrielse G, Rolston S L, Haarsma L and Kells W 1988 *Phys. Lett.* A **129** 38
[4] Robicheaux F 2004 *Phys. Rev.* A **70** 022510
[5] Nersisyan H B, Walter M and Zwicknagel G 2000 *Phys. Rev.* E **61** 7022
[6] Gabrielse G *et al* (ATHENA Collaboration) 2004 *Phys. Rev. Lett.* **93** 073401
[7] Madsen N *et al* (ATRAP Collaboration) 2005 *Phys. Rev. Lett.* **94** 033403
[8] Pohl T, Sadeghpour H R and Gabrielse G 2006 *Phys. Rev. Lett.* **97** 143401
[9] Cereceda C, de Peretti M and Deutsch C 2005 *Phys. Plasmas* **12** 022102

[10] Walter M, Zwicknagel G and Toepffer C 2005 *Eur. Phys. J.* D **35** 527
[11] Neugebauer P, Riffert H, Herold H and Ruder H 1996 *Phys. Rev.* A **54** 467
[12] Geller D K and Weisheit J C 1997 *Phys. Plasmas* **4** 4258
[13] Koryagin S A 2000 *J. Exp. Theor. Phys.* **90** 741
[14] Toepffer C 2002 *Phys. Rev.* A **66** 022714
[15] Schmidt G, Kunhardt E E and Godino J L 2000 *Phys. Rev.* E **62** 7512
[16] Hu B, Horton W, Chiu C and Petrosky T 2002 *Phys. Plasmas* **9** 1116
[17] Hu B, Horton W and Petrosky T 2002 *Phys. Rev.* E **65** 056212
[18] O'Neil T M 1983 *Phys. Fluids* **26** 2128
[19] Press W H, Teukolsky S A, Vetterling W T and Flannery B P 1992 *Numerical Recipes* 2nd edn (Cambridge: Cambridge University Press)
[20] Abrines R and Percival I C 1966 *Proc. Phys. Soc. (London)* **88** 861